Peer-reviewed version available at Nanomaterials 2019, 9, 1410; doi:10.3390/nano9101410

Article

Design of a pH-responsive conductive nanocomposite based on MWCNTs stabilized in water by amphiphilic block copolymers

Frank den Hoed[1], Andrea Pucci[2], Francesco Picchioni[1] and Patrizio Raffa[1,*]

[1]Department of Chemical Engineering – Product Technology, University of Groningen, Nijenborgh 4, 9747 AG Groningen, The Netherlands; f.m.den.hoed@rug.nl ; f.picchioni@rug.nl; p.raffa@rug.nl

[2]Department of Chemistry and Industrial Chemistry, University of Pisa, Via Giuseppe Moruzzi 13, 56124 Pisa (PI), Italy; andrea.pucci@unipi.it

Correspondence: p.raffa@rug.nl; +31503634465

Abstract

Homogeneous water dispersions of MWCNTs were prepared by ultrasonication in the presence of an amphiphilic polystyrene-block-poly(acrylic acid) (PS-b-PAA) copolymer. The ability of PS-b-PAA to disperse and stabilize MWCTNs was investigated by UV-vis, SEM and zeta potential. It is shown that the copolymer can disperse nanotubes directly by sonication in water. The results show that the addition of a styrene block to PAA enhances the dispersion efficiency compared to pure PAA, possibly due to the nanotube affinity with the polystyrene moiety. Notably, the dispersions show an evident pH-responsive behavior, being MWCNTs reaggregation promoted in basic environment. Furthermore, composites obtained by drop casting display electrical conductivity responsive to pH variations, showing the potential of such materials for sensing applications.

Keywords: Amphiphilic block copolymers; carbon nanotubes; stimuli responsive; conductive composite

1. Introduction

Carbon nanotubes (CNTs) are tube-shaped allotropes of carbon with a diameter of a few nanometers. They have received great interest since their discovery in 1991, because of their remarkable properties [1,2], in particular their mechanical strength, thermal properties and electrical conductivity [3–5]. CNTs may be used in applications like transistors, batteries, conductive films, sensors and mechanical reinforcement in composite materials [6–12]. In recent works from our research group, CNTs were used for the preparation of conductive materials responsive towards temperature changes and chemical stimuli using, respectively, functionalized polyketones [13] and pyrene-functionalized amphiphilic block copolymers [14].

Because of the high aspect ratio of CNTs, they have great van der Waals (vdW) attracting forces keeping the nanotubes in aggregated state [15] thus severely limiting possibilities to explore their full potential. CNTs dispersion in water can be of particular interest for biological applications [16] even if strongly affected by their hydrophobic nature that limits the dispersion stability over time. Notably, CNTs can form stable dispersions in some solvents with similar surface tension like NMP and DMF [17,18] even if only

Preprints (www.preprints.org) | NOT PEER-REVIEWED | Posted: 12 August 2019 doi:10.20944/preprints201908.0142.v1

Peer-reviewed version available at Nanomaterials 2019, 9, 1410; doi:10.3390/nano9101410

dilute dispersion can be made by this method. Conversely, chemical functionalization of CNTs enables the preparation of dispersions at higher concentration, and provides the possibility to attach groups with affinity for a desired dispersing medium. To make room for covalent bonds, defects on the CNT walls need to be created. This requires harsh conditions, such as high temperatures combined with highly reactive chemicals [19–21]. Disadvantages of covalent functionalization are the damaging of nanotubes during the process, with subsequent loss of favorable CNT properties, and the use of environmentally unfriendly chemicals. Alternatively, non-covalent functionalization of nanotubes is accessible as well. By this method, the surface of the nanotubes is kept intact, i.e. preserving the electrical conductivity [22]. It is worth noting that various classes of substances can be used for non-covalent stabilization of CNTs in water. A possible approach is the use of surfactants like, for example, SDS and related salts that are known to physically adsorb to the nanotube surface [23]. The hydrophobic part of a surfactant has good affinity for the nanotube wall, while the hydrophilic head promotes the dispersion in water. Affinity is best when the surfactant contains π-conjugated groups like aromatic amines, styrene or pyrene [17,24–26] that can effectively interact with the nanotubes *via* π-stacking. Moreover, the use of charged surfactants can more efficiently prevent re-aggregation of nanotubes by electrostatic repulsion. Another type of substance for nanotube stabilization are water soluble polymers. The use of polymers enables the activation of steric hindrance as an entropic (thermodynamic) stabilization mechanism in addition to the electrostatic (kinetic) repulsion [17]. The affinity for the nanotubes by water soluble polymers can be achieved by its hydrophobic backbone and rendered even more effective by the presence of π-conjugated moieties in the polymer structure (Figure 1a). Such a polymer has multiple points of interaction with the nanotubes resulting in static dispersion, which is different from the dynamic dispersion mechanism provided by surfactants (Figure 1b-d). Surfactants are more easily removed, by for example centrifugation or filtration, because of the dynamic nature of the dispersion [27,28].

(**a**) Affinity of dispersant for nanotubes can be provided by:

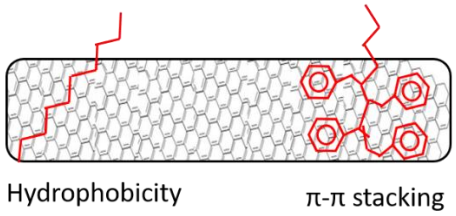

(**b**) Stabilization of the exfoliated state of the nanotubes in a dispersion is provided by:

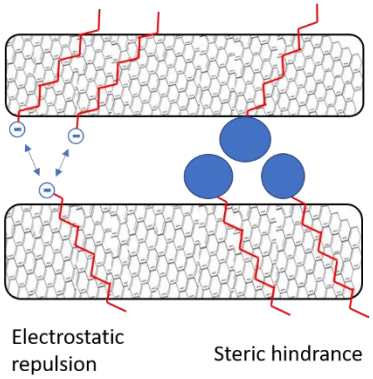

Preprints (www.preprints.org) | NOT PEER-REVIEWED | Posted: 12 August 2019 doi:10.20944/preprints201908.0142.v1

Peer-reviewed version available at Nanomaterials 2019, 9, 1410; doi:10.3390/nano9101410

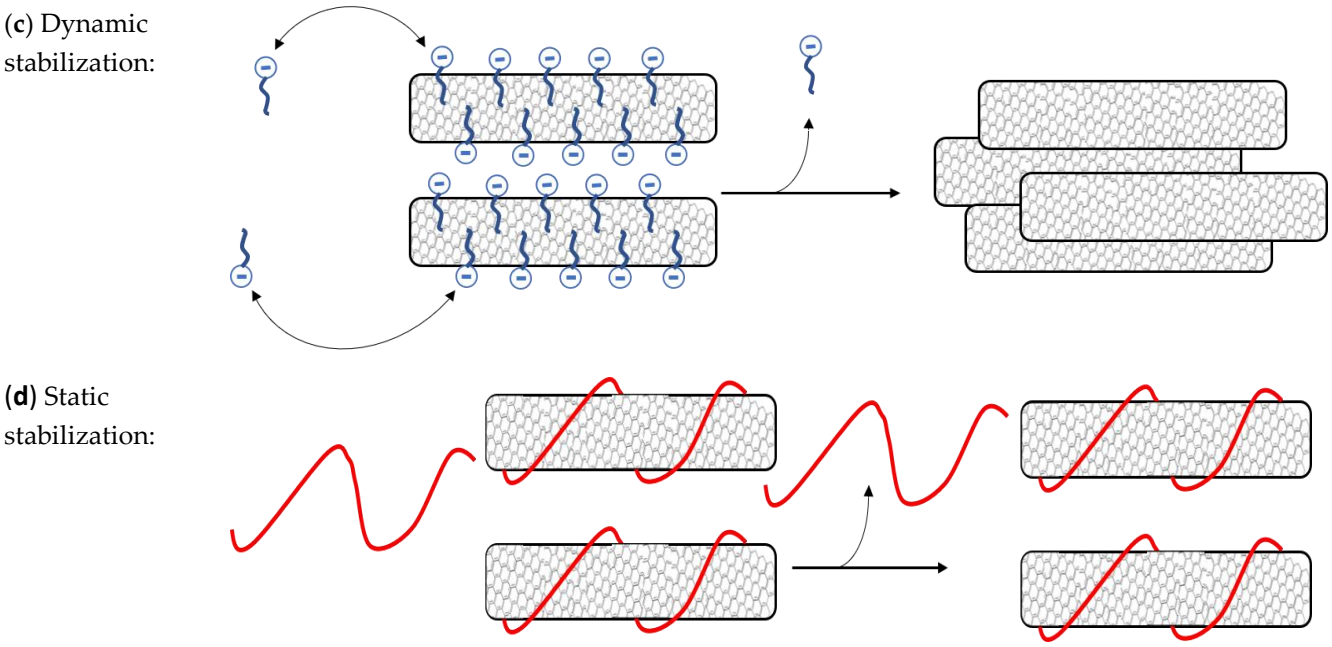

Figure 1. (**a**) Affinity of a dispersant for nanotubes can be provided by hydrophobicity, but even better by π-conjugated compounds that can stack on the nanotubes by π-π interactions. (**b**) There are two mechanisms that can prevent nanotube reaggregation. Firstly, electrostatic charges on the dispersant that repulse dispersants on other nanotubes. Secondly, bulky groups can hinder nanotubes from getting close to each other. (**c**) Surfactants and small molecules are stabilized dynamically. Dispersants can exchange easily from nanotube wall to solvent. These dispersants are removed more easily resulting in reaggregation. (**d**) Larger polymers with high nanotube affinity can wrap around the nanotubes resulting in static stabilization where no exchange of dispersants takes place. These are harder to remove and can stabilize nanotubes in conditions like centrifugation, filtration, dialysis and precipitation.

It is further reported that when the substance used for stabilization is responsive to external stimuli, this enables the possibility of making a smart material with sensor abilities [29]. Polyelectrolytes for example are water soluble polymers responsive to pH and salinity due to their large number of ionizable groups. [30] Poly(acrylic acid) (PAA) has been shown to effectively disperse nanotubes in water [31,32] depending on pH. At high pH (>8) PAA contains many charged groups which significantly decrease the affinity for CNT and thus decreases the CNT dispersion abilities [32–34]. The affinity could be improved by attaching a π-conjugated moiety, like polystyrene (PS), to the PAA chain as this allows for π-π non-covalent bonds. A copolymer of PAA and polystyrene should therefore result in more stable dispersions which is more static (Figure 1). PS-PAA block copolymers are known to form colloidal gels sensitive to external stimuli such as pH and salinity [35–38]. The dispersion stability compared to PAA could be significantly improved by micelle formation around the CNT, as it has been shown in water/DMF solution for cross-linked PS-b-PAA in a study by Kang and Taton [39]. In the mentioned study, the stabilization of CNTs in solution is demonstrated, but no composites were prepared and no investigation of the responsive properties has been performed. Better control and higher stability in aqueous CNT dispersions combined with responsive properties are of vital importance to explore the full potential of CNTs and use them as smart materials.

Herein, we propose to study the preparation of multi-walled CNTs (MWCNTs) dispersions directly stabilized in water by means of several PS-b-PAA copolymers with variable length of the PAA block. The

PAA length is varied because it governs conformational changes with pH variations [40], and it is maintained several times longer than the PS chain to provide the copolymers water solubility. The copolymers were prepared by ATRP [41], according to previously published procedure [36]. ATRP allowed for precise design of the polymer, control over block length and narrow molecular weight distribution. First, a polystyrene macroinitiator was synthesized and chain extended with tert-butyl acrylate, which was eventually hydrolyzed to yield the PAA block. The two-step approach for the attachment of the PAA chain is required because polymerization control is poor for copper-mediated ATRP in protic environments [42].

MWCNTs/PS-b-PAA copolymer dispersions were prepared by ultrasonication and their pH-responsive behavior studied by spectroscopy and microscopy investigations. Furthermore, solid composites realized by drop casting were studied in terms of their electrical-responsiveness towards pH variations.

2. Materials and methods

2.1 Materials

Multi-walled carbon nanotubes (CNTs) were bought from Sigma-Aldrich (product number: 791431, lot MKBT4011V). They were used without any further purification. Methyl 2-bromopropionate (Sigma-Aldrich, ≥99%), Styrene (Sigma-Aldrich, ≥99%), N,N,N′,N″,N″-Pentamethyldiethylenetriamine (Sigma-Aldrich, 99%), Anisole (Sigma-Aldrich, 99.7%), Glacial acetic acid, methanol, dioxane, THF, DMF, Ethanol, Ethyl acetate, 1,4-diazabicyclooctane were used without any purification. Tert-Butyl acrylate (Sigma-Aldrich, 98%) was purified over a column of basic aluminum oxide and stored under nitrogen before use. Copper(I)Bromide (Sigma-Aldrich,99%) and Copper(I)Chloride (Sigma-Aldrich,99%) were stirred in glacial acetic acid for 5 hours, filtered, washed with acetic acid, ethanol and ethyl acetate, and dried under vacuum before use.

2.2 Polymer preparation

The styrene macroinitiator (PS-Br) was prepared by the following procedure: 5-10 mmol MBP, 5 mmol Cu(I)Br, 300 mmol styrene was dissolved in 20 mL anisole in a 250 mL three-necked round bottom flask. The flask was placed in an oil bath at 100 °C. Air was removed by bubbling nitrogen gas through the solution for at least 30 minutes. Then, 10 mmol of PMDETA were added to start the reaction. After 5 hours, the reaction was stopped by cooling down, introduction of air and dilution with 50-100 mL THF. The copper catalyst was removed by filtration over a neutral alumina column. The solution was precipitated in an excess of methanol, filtered, redissolved in THF, reprecipitated in methanol:water (2:1 v/v), washed with methanol and dried overnight at 60 °C. A white solid was obtained. The molecular weight of the polymer was determined by NMR and GPC.

To prepare the second block of the polymer, 1 g of macroinitiator (PS-Br) was dissolved in 15 mL anisole under nitrogen. Cu(I)Cl and monomer (tBA) were added according to the desired stoichiometry. The flask was placed in an oil bath at 90 °C and nitrogen was bubbled through the solution for at least half an hour before PMDETA was added. The reaction was stopped after a given time by cooling to room temperature, introducing air and 50 mL THF. The copper catalyst was removed by filtration over a neutral alumina column. The solution was precipitated in an excess of methanol:water (2:1 v/v), filtered, redissolved in THF,

reprecipitated in methanol:water (2:1), washed with methanol and dried overnight at 60^{0}C. A white solid was obtained. The molecular weight of the polymer was determined by NMR and GPC.

The resulting polymers were hydrolyzed in a 1,4-dioxane solution in a round-bottom flask. Approximately 20 mL per gram polymer was used. The flask was equipped with a stirring egg, a reflux condenser and was heated to 100 ^{0}C in an oil bath. After an hour, HCl was added (2 mL more than stoichiometrically required). The reaction was stopped after 3 hours by cooling down. The solution was precipitated in acetone, filtered and dried at 60 ^{0}C. The extent of hydrolysis was determined by NMR in DMSO-d6.

2.3 Characterization

For GPC measurements a solution of 5 mg/mL polymer in THF was prepared. Toluene was used as a reference. The eluent ran at 1 mL/min. The GPC had a LC1240 Refractive index detector and 3 PL-gel 3 μm Mixed-E columns. To determine the length of a polymer consisting only of tBA blocks, a GPC with triple detection was used: a Viscotek Rals detector, a viscometer H502 and a shodex RI-71 refractive index detector with one guard column (PL-gel 5 μm Guard, 50 mm) which is followed by two columns of PL-gel 5 μm Mixed-C, 300 mm). A dn/dc value of 0.0479 mL/g was used for the tBA chains.

1 mg of MWCNTs and 15 mg of polymer were added to 3 mL water in a 20 mL vial. The mixture was ultrasonicated for 5 minutes in a Hielscher UP400S at 60% power 0.5 s^{-1} frequency. The dispersion was diluted with water to a polymer concentration of 0.46 mg/mL and (if pH was adjusted) a 1M NaOH solution was added dropwise until the desired pH was measured. This was sonicated for another 3 minutes, centrifuged at 3000 rpm and filtered before being characterized. For samples with different nanotube concentrations, the amount of nanotubes was varied while the polymer concentration and liquid volume was kept constant.

The light absorption of the prepared dispersion was determined from wavelength 300 to 600 nm using a PerkinElmer Lambda 650 spectrometer and 1 cm cuvette.

The zeta potential of the dispersions was measured to determine the suspension stability. The zeta potential was measured by Brookhaven ZetaPALS. 10 cycles were performed per sample. A polymer concentration of 6 mg per mL MiliQ water was used. For samples containing MWCNTs, a feed of 0.22 mg/mL nanotubes was used.

The morphology of the solid dispersions was further investigated by FEI Quanta 450 FEG Environmental Scanning Electron Microscope (SEM) pictures. The MWCNTs/polymer samples for SEM were ultrasonically dispersed in water for analysis. The suspensions were deposited on a gold-coated silicon wafer and allowed to dry in a vacuum system overnight. The wafer was then mounted onto a stainless steel sample holder using carbon tape.

For dried samples, water/polymer/nanotube dispersions were prepared with different CNTs content. 25 μL of each dispersion was drop casted directly on the electrodes. Water was evaporated by drying in a 120 ^{0}C oven for 5 minutes. Electrodes were bought from CAD Line, Pisa, Italy. The electrodes were fabricated onto FR-4 that is a composite material composed of woven fiberglass cloth with an epoxy resin binder substrate (thickness of 2 mm). Copper tracks were obtained by photolithography and electroplated with nickel and gold to fabricate the electrodes (thickness of copper 35 μm, nickel 3.0 μm, and gold 1.2 μm). The electrical

Peer-reviewed version available at Nanomaterials 2019, 9, 1410; doi:10.3390/nano9101410

resistance of the electrode was measured using a Keithley 2000 multimeter. To determine the weight percentage of nanotubes in the polymer composite, TGA measurements were performed in a Mettler Toledo TGA/SDTA851 from 25 ^{0}C to 450 ^{0}C.

The pH response was further investigated by experiments with an organic base. The electrodes with drop casted films were used. These were submerged in an acetone solution, which is a non-solvent, containing a concentration of 5 g/L 1,4-Diazabicyclo[2.2.2]octane (DABCO, pKa = 8.82) [43]. The electrodes were removed from the acetone/DABCO solution after 15 minutes and dried at room temperature for 24 hours. Subsequently, the electrical resistance was measured by means of the Keithley 2000 multimeter.

3. Results and discussion

3.1 Polymer/MWCNT dispersion in water

Several polymers were designed and synthesized by the procedure that is shown in Figure 2. The length of the blocks is expressed in the sample name. For example, $PS_{26}PAA_{81}$ is a diblock copolymer consisting of a polystyrene chain of 26 units and a polyacrylic acid chain of 81 units (approximately). Details of synthesis and characterization can be found in the supporting information section. The relatively short hydrophobic block (26 units) combined with a long hydrophilic block allowed for the polymers water solubility.

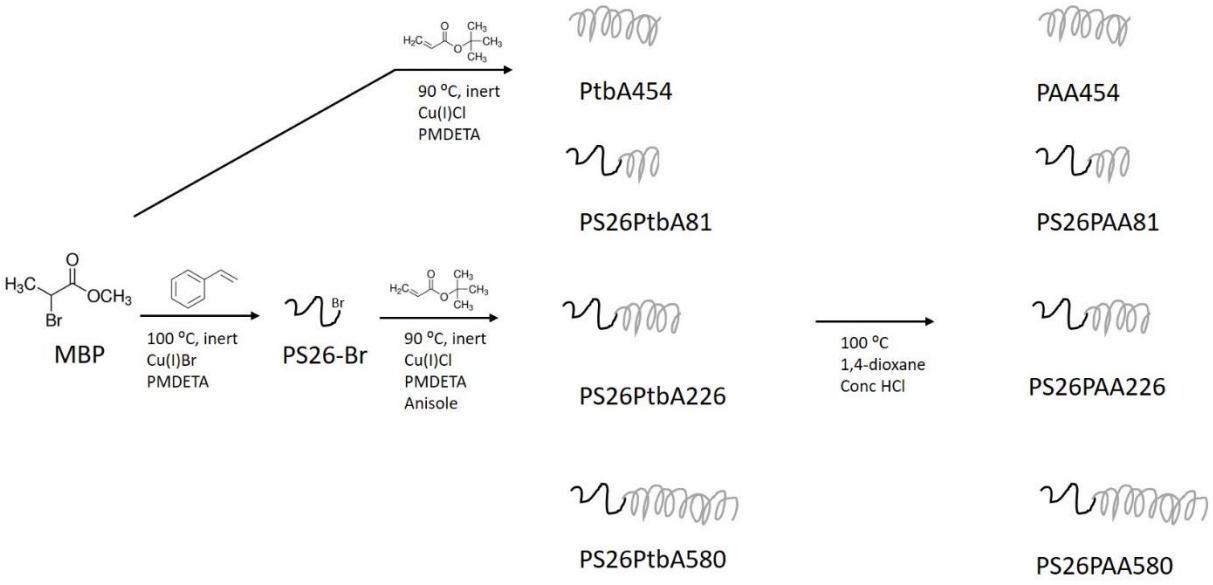

Figure 2. Process design for the synthesis of amphiphilic block copolymers used for the dispersion of MWCNTs. In the first step a polystyrene macroinitiator was made. Secondly, a chain of tert-butyl acrylate was formed in various lengths. The tBA groups were eventually hydrolised to form acrylic acid moieties.

The copolymers were dissolved in water (0.46 mg/mL) and the CNTs dispersed by ultrasonication for 5 minutes (0.03 mg/mL feed). After possible pH-adjustment, samples were sonicated for another 3 minutes. To estimate the amount of MWCNTs effectively stabilized by the prepared copolymers at different pH, UV spectra of the dispersion (after centrifugation to remove the non-stabilized MWCNTs) were recorded (Figure 3). The amount of light absorbed or scattered by a dispersion is correlated to the MWCNTs

Preprints (www.preprints.org) | NOT PEER-REVIEWED | Posted: 12 August 2019 doi:10.20944/preprints201908.0142.v1

Peer-reviewed version available at Nanomaterials 2019, 9, 1410; doi:10.3390/nano9101410

concentration [34]. The intensity at a given arbitrary wavelength (450 nm) would be proportional to the amount of MWCNTs present in the dispersion, according to the Lambert-Beer law. In Figure 4, the light absorption at 450 nm is shown for polymer/nanotube dispersions in water at various pH and for different polymers.

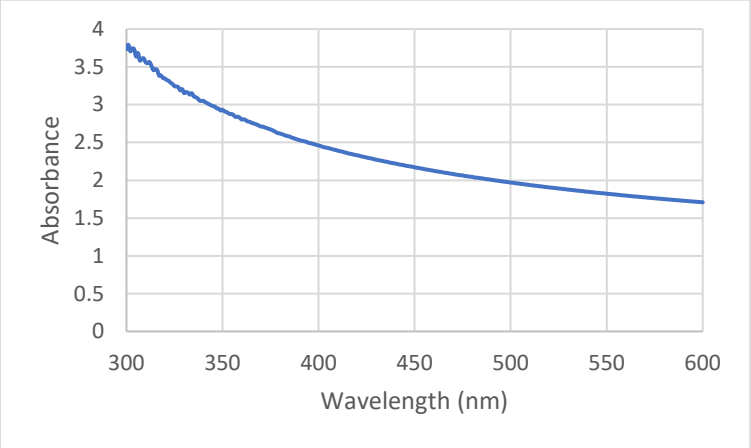

Figure 3. Example of UV-vis spectrum recorded from 300 to 600 nm of MWCNTs (feed of 0.03 mg/mL) dispersed in $PS_{26}PAA_{226}$ water solution (0.46 mg/mL, pH 5).

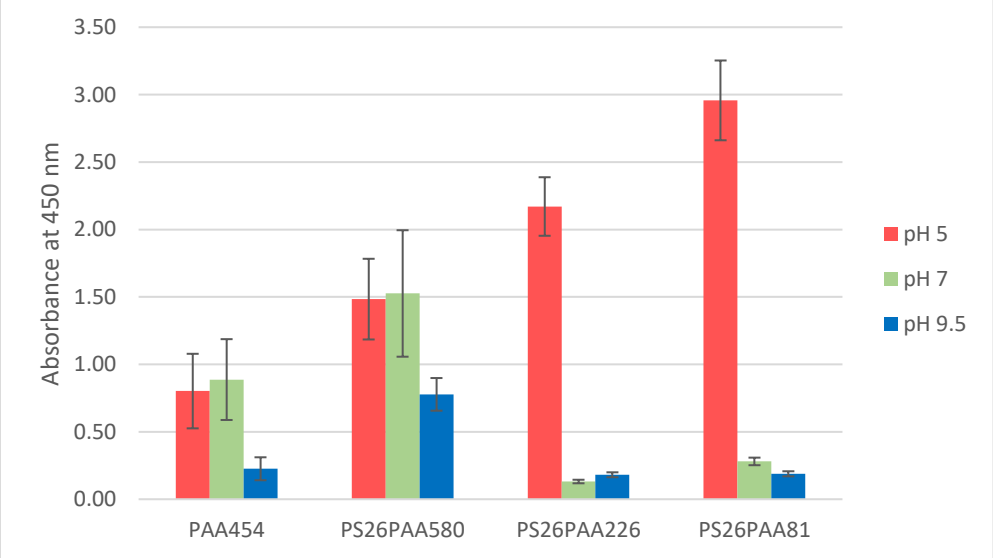

Figure 4. Absorbances values at 450 nm recorded from different polymer dispersions at three diverse pH.

Since all dispersions contain the same copolymer mass, the shorter chains have a higher molar concentration. Longer chains compensate this feature due to their size, which was estimated by calculating the total surface coverage of PAA in the solution. It was assumed that the polymers adsorb on the CNTs surface as single chains, schematically visualized in Figure 5, allowing calculation of the radius of gyration (see supporting information) and the corresponding surface area of the single PAA block. This was eventually multiplied by the molar concentration of the polymer to find the total coverage area of PAA per mL of dispersion. The calculated total surface coverage for each sample is given in Table 1.

Preprints (www.preprints.org) | NOT PEER-REVIEWED | Posted: 12 August 2019 doi:10.20944/preprints201908.0142.v1

Peer-reviewed version available at Nanomaterials 2019, 9, 1410; doi:10.3390/nano9101410

Table 1. Total surface coverage of single polymer PAA chain for different polymers at 0.46 mg/mL concentration in water at pH 5.

Polymer	Concentration (mmol/mL)	Total surface coverage PAA (m^2/mL)
PAA_{454}	1.41E-05	917
$PS_{26}PAA_{81}$	5.38E-05	649
$PS_{26}PAA_{226}$	2.42E-05	795
$PS_{26}PAA_{580}$	1.03E-05	864

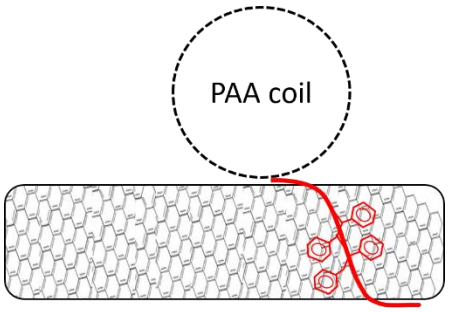

Figure 5. Schematic visualization of single chain adsorption on nanotube surface.

Without pH adjustment, the pH of the dispersion was 5 for all polymers. At this pH the pure PAA polymer has the lowest light absorption compared to the rest of the set of polymers and thus has the lowest dispersion efficiency (Figure 4). This means that the polymer with the highest surface coverage of PAA according to Table 1, has the worst dispersion while the polymer with the smallest surface coverage provides the highest nanotube concentration. This polymer, $PS_{26}PAA_{81}$ has the highest relative polystyrene content, that should contribute with a more effective π-π interaction with the CNTs. This suggests that the overall CNT/polymer affinity is more limiting than the stabilizing effects provided by the PAA chains. The assumption of single chain adsorption in spherical form used for the model in Table 1 and Figure 5 is therefore too simplistic.

The polymers used in this study are indeed known to form colloidal micellar aggregates in water, as we have discussed in previous research [35–38]. If the polymers would form micelles around the MWCNTs like surfactants do [44] (PS/nanotube forming the core and PAA the corona as is visualized in Figure 6), the PAA length would not make a difference as it merely determines the thickness of the protecting layer

Preprints (www.preprints.org) | NOT PEER-REVIEWED | Posted: 12 August 2019 doi:10.20944/preprints201908.0142.v1

Peer-reviewed version available at Nanomaterials 2019, 9, 1410; doi:10.3390/nano9101410

between nanotube and water. As long as this is thick enough, the molar concentration of the polymer would be determining the amount of nanotubes that can be dispersed. Based on these considerations, we can suggest that in our system, the sonication partially disrupt the polymeric micellar aggregates and causes a rearrangement of polymeric chains around the CNTs, based on their affinity for the polystyrene block.

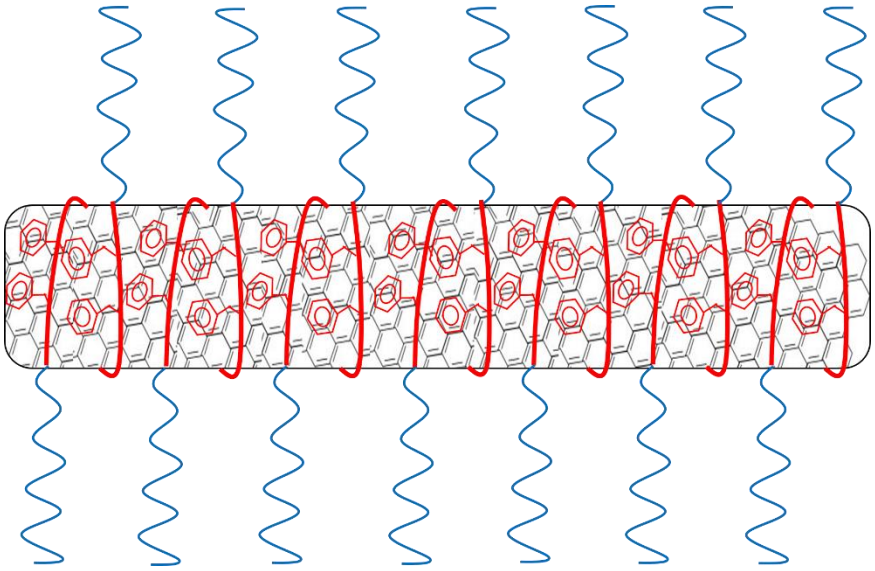

Figure 6. Schematic visualization of micelle encapsulation of nanotubes by the amphiphilic polymer.

To make things more complicated, the PAA chain conformation is also dependent on its degree of protonation, therefore on the solution pH. At low pH, PAA is mostly present in coiled formation [45–47] and shorter chains only have a slightly smaller radius compared to the longer ones. Therefore, they can cover a larger amount of the nanotube surface at the same polymer weight concentration (meaning higher molar concentration).

Another point to consider, is that while π-π interaction allows the polymer to wrap around the nanotube, when PAA is slightly deprotonated (between pH 5 and 7) it rather assumes a more stretched conformation and is only partially in contact with the nanotube. The weakly ionized polymer can non-covalently bind to the nanotube surface [32].

The pK_a of acrylic acid is 4.25 and approximately 4.5 for polyacrylic acid [40]. When the pH is adjusted from 5 to 7 and 9.5 the PAA chain in the polymer becomes deprotonated. This causes intramolecular repulsions between charged units resulting in an increase of the radius of gyration [46]. The conformation of the polymer changes from coiled to elongated. If a micellar structure is formed around the nanotubes, this would increase the thickness of the PAA layer and improve stabilization. Figure 4 shows the amount of CNTs stabilized at various pH by the 4 studied copolymers. The results show that less nanotubes are dispersed at higher pH, especially for the shortest PAA chains, thus suggesting that the stabilization has become weaker. Therefore, this behavior contradicts the hypothesis of a micellar structure around the nanotubes.

Preprints (www.preprints.org) | NOT PEER-REVIEWED | Posted: 12 August 2019 doi:10.20944/preprints201908.0142.v1

Peer-reviewed version available at Nanomaterials 2019, 9, 1410; doi:10.3390/nano9101410

The stabilization mechanism of pure PAA in water has been hypothesized by Erika et al to form globular structures parallel to the surface of the nanotubes [32–34]. The mentioned research also found a decrease in nanotubes dispersed at high pH as the conformation of the polymer changes from globular to stretched (still parallel to the nanotube surface). In contrast with a micelle model, where stretching of the polymer leads to increased steric hindrance (Figure 4), the conformation change according to this model leads to less steric hindrance and thus less nanotubes dispersed (Figure 7). The increase in electrostatic repulsion as a stabilization mechanism is not enough to compensate for reduced steric hindrance, possibly because the lower acid character of the polymer investigated in this study. As the number of charges on the PAA chain increase, the PAA chain becomes less hydrophobic and therefore loses affinity for the nanotubes wall. Detaching during sonication thus becomes more likely, despite the strong MWCNT-affinity of the PS block. Although we have no direct evidence for the model in Figure 7, our data does not contradict this hypothesis.

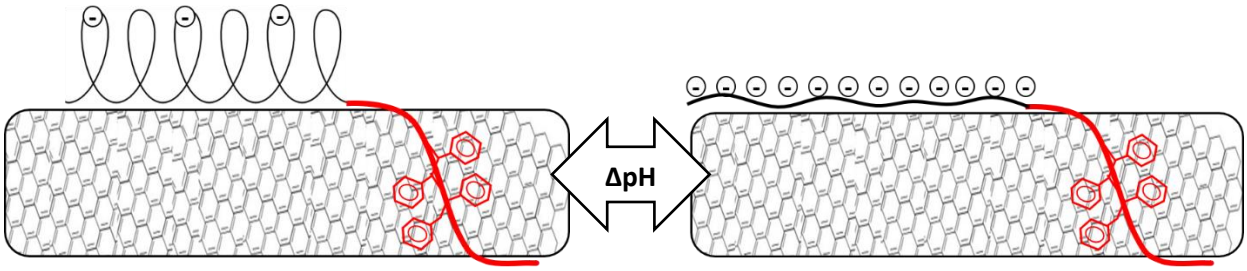

Figure 7. Schematic visualization of the consequences of pH change. The conformation of PAA changes from globular to rod-like resulting in reduced steric hindrance between the nanotubes.

According to our data, the affinity of the polymer for the nanotube is the limiting factor at low pH, whereas at high pH, the stabilizing ability of PAA decreases and becomes the limiting factor. Therefore, high styrene content leads to highest nanotube concentration at low pH and high PAA content leads to highest nanotube concentration at high pH.

$PS_{26}PAA_{580}$, i.e. the polymer sample with the best nanotube stabilization efficiency at high pH, was analyzed in terms of zeta potential measurements (Table 2). Since a high absolute zeta potential value (>25 mV or <-25 mV) indicates good colloidal stability [32], the zeta potential at pH 5 is too small for stable colloidal dispersion, thus meaning that micelle encapsulation is indeed unlikely. Conversely, the zeta potential is high enough at pH 9.5 for the formation of stable colloids. In both cases, the incorporation of CNTs seems to reduce the micelle stability of the system.

These findings suggest a shift in dispersion stabilization mechanism from steric hindrance to electrostatic repulsion. As shown by the zeta potential data (Table 2), $PS_{26}PAA_{580}$ is almost uncharged at pH 5, making it unable to stabilize a nanotube dispersion by the electrostatic repulsion mechanism. Steric hindrance is in this environment the only stabilization mechanism. At high pH, the zeta potential is -58 mV, suggesting very good colloidal stability which enables electrostatic repulsion as a stabilization mechanism. However, Figure 4 also shows that the amount of nanotubes dispersed decreases with pH raising. This can be explained by the increase in charge density in the PAA chain, which has two effects. Firstly, the PAA chain becomes less hydrophobic and therefore loses affinity for the nanotube wall. Detachment during sonication thus becomes more likely, despite the strong affinity of the PS block. Secondly, the increase in charge density on the PAA causes a conformational change, as illustrated before (Figure 7). This severely reduces the steric hindrance. Especially dispersions containing polymer with short PAA chain ($PS_{26}PAA_{226}$ and $PS_{26}PAA_{81}$)

Preprints (www.preprints.org) | NOT PEER-REVIEWED | Posted: 12 August 2019 doi:10.20944/preprints201908.0142.v1

Peer-reviewed version available at Nanomaterials 2019, 9, 1410; doi:10.3390/nano9101410

show a sharp decrease in absorbance (Figure 4), which is already found at pH 7. These short chains have less random walk steps and thus are already in rod shape conformation at pH 7. Longer chains, can still make a highly stretched coil and therefore provide steric hindrance.

Table 2. Zeta potential of polymer samples in water (6 mg/mL). MWCNTs were added for some samples with a feed of 0.22 mg/mL. 10 cycles were performed.

Sample	pH	Zeta potential
$PS_{26}PAA_{580}$	5	-15 mV
$PS_{26}PAA_{580}$ with MWCNTs	5	-7 mV
$PS_{26}PAA_{580}$	9.5	-66 mV
$PS_{26}PAA_{580}$ with MWCNTs	9.5	-58 mV

The nanotube dispersions were analyzed by SEM in both acidic and alkaline environments aimed at supporting the observations gathered from UV-Vis spectroscopy. In acidic conditions, the $PS_{26}PAA_{226}$ composite (Figure 8a) shows well separated CNTs structures thus suggesting their homogeneous distribution in the original dispersion before drying. In alkaline conditions, nanotubes were mostly aggregated (Figure 8b), which is a result of the conformational change of the polymer as hypothesized in Figure 7. Notably, in UV-Vis measurements, aggregated nanotubes were separated by centrifugation from the analyzed dispersion, thus explaining the low absorbance value for alkaline $PS_{26}PAA_{226}$ in Figure 4. Similarly, for $PS_{26}PAA_{580}$ a decrease nanotubes dispersed is found when the pH is increased from 5 to 9.5. However, differently from $PS_{26}PAA_{226}$, the decrease is much less severe, because Figure 8e and 8f still show nanotubes homogeneously dispersed suggesting good stability of the remaining nanotubes. The SEM images confirm the observations made with UV-vis (Figure 4), because this also showed a milder response for longer PAA chains. In summary, the micrographs in Figure 8 are a visual evidence of the pH-responsive stabilization of MWCNTs in water that is easily modulated by tuning the length of the PAA chain.

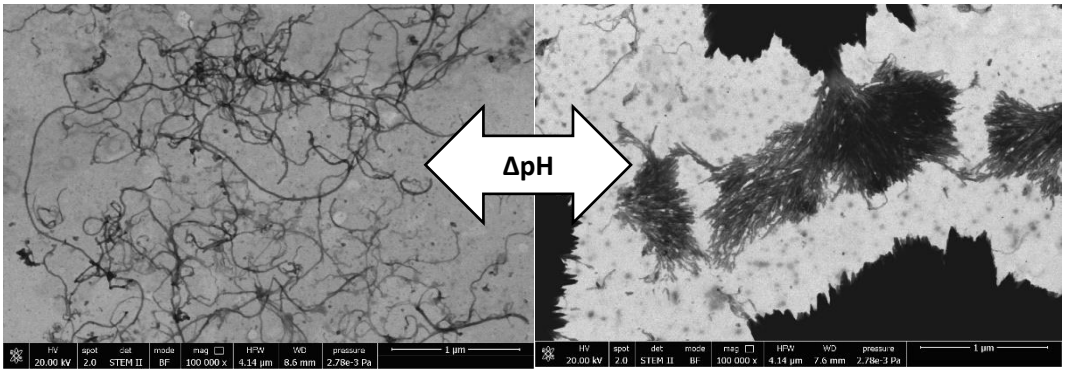

(**a**) (**b**)

Preprints (www.preprints.org) | NOT PEER-REVIEWED | Posted: 12 August 2019 doi:10.20944/preprints201908.0142.v1

Peer-reviewed version available at Nanomaterials 2019, 9, 1410; doi:10.3390/nano9101410

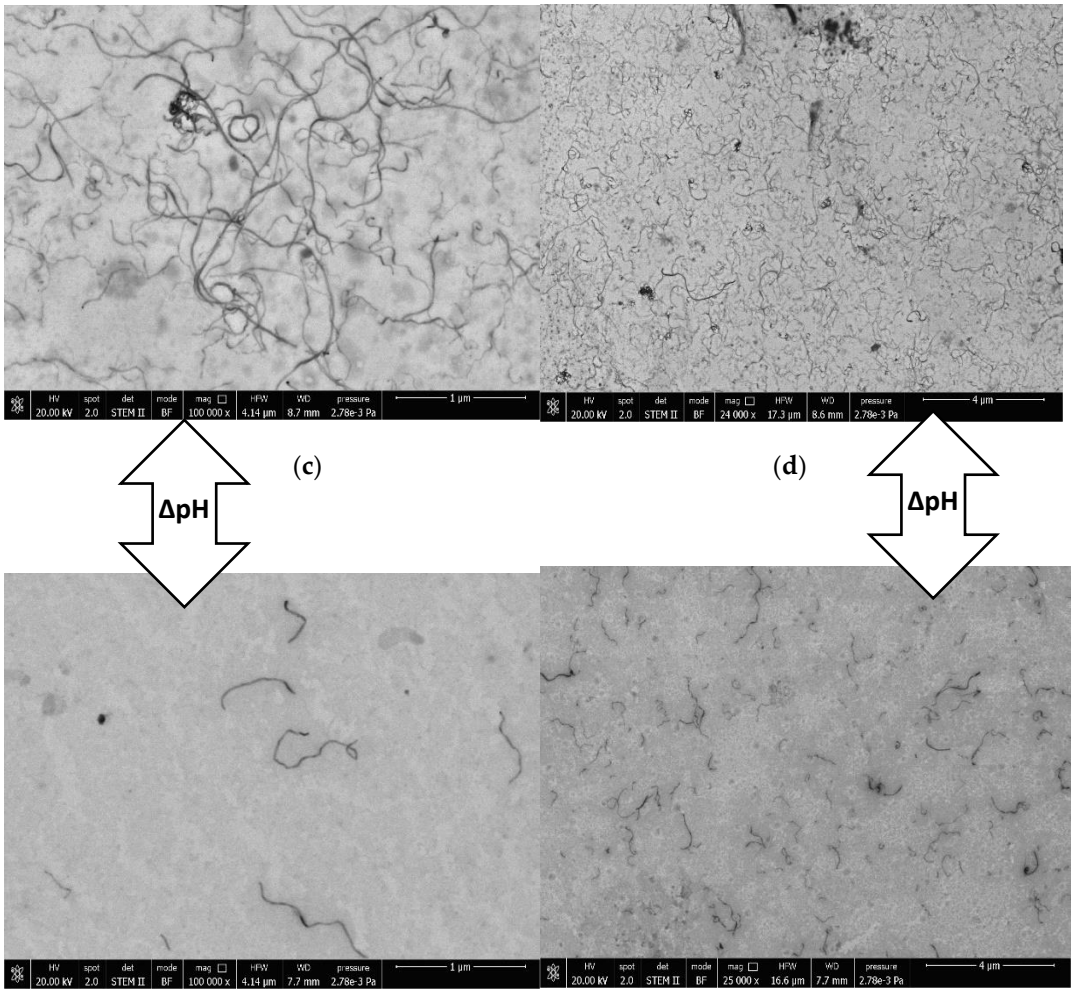

Figure 8. Field emission scanning electron micrographs of (**a**) $PS_{26}PAA_{226}$ pH 5, (**b**) $PS_{26}PAA_{226}$ pH 9.5, (**c**) and (**d**) $PS_{26}PAA_{580}$ pH 5, (**e**) and (**f**): $PS_{26}PAA_{580}$ pH 9.5.

Preprints (www.preprints.org) | NOT PEER-REVIEWED | Posted: 12 August 2019 doi:10.20944/preprints201908.0142.v1

Peer-reviewed version available at Nanomaterials 2019, 9, 1410; doi:10.3390/nano9101410

3.2 Resistivity of MWCNTs/polymer composites

The resistive behavior of the MWCNTs/polymer composites was eventually evaluated by depositing water dispersions containing different MWCNTs content on an electrical circuit. The MWCNT content of the solid samples was estimated by using TGA (see supporting information) by plotting the relative residue mass at 450 °C as a function of the alimentation content (Figure 9). A logarithmic empirical fit of the experimental data was used to determine the actual MWCNTs weight percentage in the composites (Figure 9).

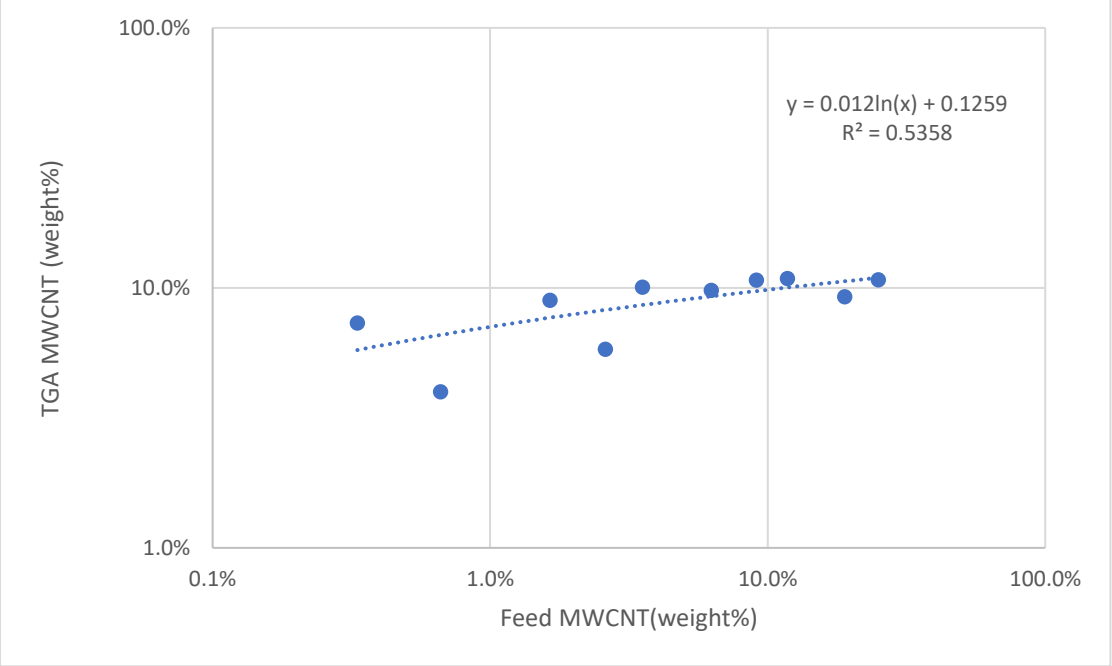

Figure 9. Correlation between wt% fed to a dispersion and the wt% measured using TGA

The $PS_{26}PAA_{580}$ copolymer was selected since it provided the best dispersions at high pH. After drying the MWCNTs/$PS_{26}PAA_{580}$ composite in an oven, the electrical resistance of the electrode was measured at room temperature and plotted (Figure 10) against the MWCNTs weight percentage calculated according to Figure 9. For alkaline samples, 1M NaOH was added dropwise to the same dispersions until the desired pH was measured. This means that alkaline samples had the same CNTs concentration after drying. The electrical resistance was eventually measured on three replicates.

For conductive fillers in an insulating matrix, the conductance depends on the percolative networks among the nanotubes. The percolation threshold (critical filler content where resistance sharply decreases) [48] of a composite can be found by fitting the experimental data with the equation 1 [49].

$$R \propto \frac{1}{(\phi-\phi_p)^t} \quad (1)$$

where R is the resistance of the composite, Φ is the filler content, Φ_p is the filler content at the percolation threshold and t is the critical exponent which is non-universal.

Figure 10 shows that alkaline samples display lower electrical resistance than the acidic ones, with a percolation threshold of approximately 8.2 wt% for the former and 9.3 wt% for the latter composites. This feature suggests that the composites obtained from alkaline dispersions possibly contains MWCNTs in

Preprints (www.preprints.org) | NOT PEER-REVIEWED | Posted: 12 August 2019 doi:10.20944/preprints201908.0142.v1

Peer-reviewed version available at Nanomaterials 2019, 9, 1410; doi:10.3390/nano9101410

closer proximity to each other, in agreement with microscopy investigations. Nevertheless, an effective contribution of the charge density on the electrical conductivity of MWCNTs dispersions cannot be neglected [50,51].

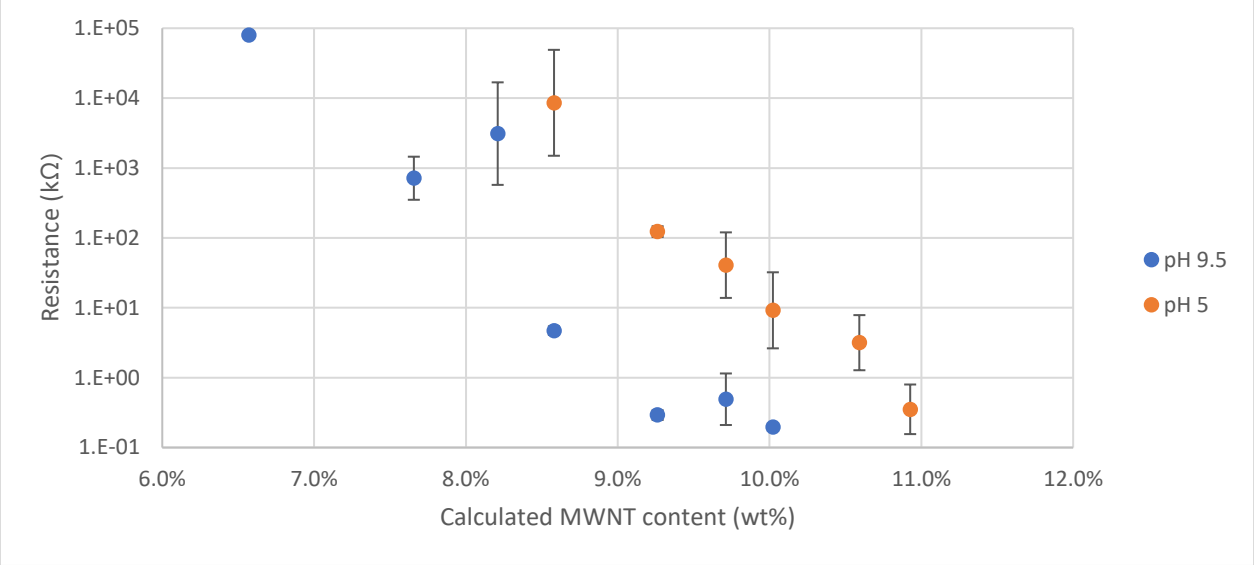

Figure 10. The electrical resistance of composites made from $PS_{26}PAA_{580}$ polymer. Increasing the wt% of MWCNTs results in reduced resistance. For every sample an acidic (pH 5) and alkaline (pH 9.5) composite was made.

These experiments well evidence the pH-responsive behavior of the MWCNTs/polymer composites. This behavior inspired us to carry out further studies aimed at determining the possible influence of the resistive character of the composite even in the solid state by means of an organic base dissolved in acetone, i.e. a non-solvent for the polymer. DABCO (pK_a is 8.82) was selected as the organic base since is able to neutralize the acidic groups of the PAA block (pK_a of acrylic acid monomer is 4.25) of $PS_{26}PAA_{580}$ copolymer. The electrodes with drop casted CNTs/$PS_{26}PAA_{580}$ sample were submerged in an acetone solution containing 5 g/L (0.45 mol/L) DABCO for half an hour. Indeed, a significant decrease in electrical resistance was found after immersion for 15 minutes (Figure 11), thus suggesting that the polymer microstructure can be altered even when deposited on a solid support. After removal from the acetone solution, the electrical resistance value suddenly spikes to very high values, possibly due to a quick drop in temperature, due to solvent evaporation. The effect of temperature on the resistivity is not surprising since CNTs are known to be sensitive to temperature variations [52,53].

The electrical resistance reaches then a stable value only after 24 hours out of the acetone solution. A possible explanation for this behavior is that water might have been removed from the composite by acetone. Since PAA is hygroscopic, the composite can slowly reabsorb water from atmospheric humidity. This suggests that absorbed water plays a role in the microstructure (and thus electrical resistance) of the composite. Notably, humidity sensor made by using PAA have been effectively proposed in the literature by Wu et al [54].

Preprints (www.preprints.org) | NOT PEER-REVIEWED | Posted: 12 August 2019 doi:10.20944/preprints201908.0142.v1

Peer-reviewed version available at Nanomaterials 2019, 9, 1410; doi:10.3390/nano9101410

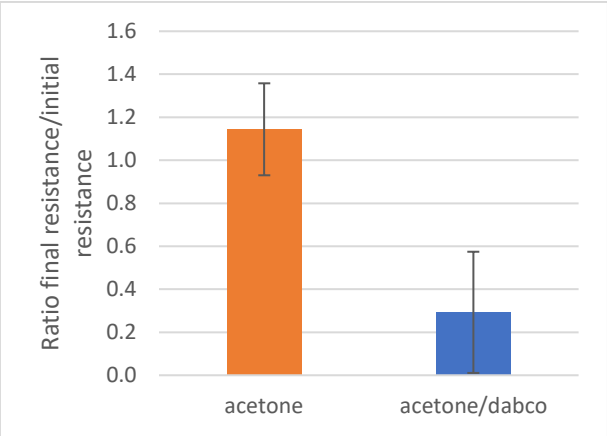

Figure 11. Composites dried on electrodes were submerged in acetone or in a DABCO solution in acetone (0.45 mol/L). After taking them out and waiting 24 hours, the electrical resistance was compared with the original resistance from which a ratio was calculated. The average of 4 measurements is reported.

4. Conclusions

In this study, a series of pH responsive amphiphilic PS-b-PAA copolymers with variable length of the PAA block were successfully synthesized. The polymers were found to be able to disperse MWCNTs directly by sonication in water to a different extent, depending on their composition. UV-Vis and SEM investigations reported that PS-b-PAA copolymers with larger relative content of styrene units were able to better disperse carbon nanotubes in water, thanks to the chemical affinity between the aromatic moieties of the polymer and the graphitic nature of MWCNTs. Notably, the dispersion stability was also affected by pH, which was evidenced by a change in absorption in UV-vis experiments and a decreased number of nanotubes visible on SEM micrographs. The stabilization ability of all polymers was higher at lower pH values possibly due to conformational changes of the PAA block, resulting in a different stabilization mechanism. At low pH, the stabilization mechanism is likely based on steric hindrance, since the zeta potential is too low for the alternative mechanism, electrostatic repulsion. Deprotonation of PAA at high pH causes improved electrostatic repulsion as evidenced by the higher zeta potential, but at the same time the charges on the polymer reduce the affinity for the nanotubes. Furthermore, the hypothesized globule to stretched conformational change parallel to the nanotube surface reduces steric hindrance, resulting in the overall decrease in CNTs stabilization.

Solid dispersions of the prepared composites resulted in electrically-conductive mixtures, with composites obtained from alkaline dispersion displaying lower percolation thresholds. This pH-dependent behavior was tentatively explained in terms of conformational changes of PAA from globule to stretched, which decreases the steric hindrance between the nanotubes and favors the formation of effective percolative networks. Moreover, by exposing the solid composite to an organic base dissolved in acetone, the resistance was found to drop, illustrating the potential of these systems for sensing applications.

Overall, this paper evidenced the versatility of the prepared polymers in providing liquid or solid CNTs dispersions directly in water, with pH-response tuned by the block lengths of the amphiphilic polymer. This feature is merely illustrative, but it was designed to stimulate the exploration of novel possibilities to tailor and manage the electrical conductance of polymeric materials, having in mind possible applications

where a pH-dependent electrical response is relevant, such as, for example, the design of sensors, wearable electronics, or bio-inspired smart materials.

Supplementary Materials:

Attached supporting information file which contains references [40,55–57].

References

1. Iijima, S. Helical microtubules of graphitic carbon. *Nature* **1991**, *354*, 56–58.

2. Volder, M.F.L. De; Tawfick, S.H.; Baughman, R.H.; Hart, A.J. CNTs: Present and Future Commercial Applications. *Science (80-.).* **2013**, *339*, 535–539.

3. Wei, B.Q.; Vajtai, R.; Ajayan, P.M. Reliability and current carrying capacity of carbon nanotubes. *Appl. Phys. Lett.* **2001**, *79*, 1172–1174.

4. Peng, B.; Locascio, M.; Zapol, P.; Li, S.; Mielke, S.L.; Schatz, G.C.; Espinosa, H.D. Measurements of near-ultimate strength for multiwalled carbon nanotubes and irradiation-induced crosslinking improvements. *Nat. Nanotechnol.* **2008**, *3*, 626–631.

5. Pop, E.; Mann, D.; Wang, Q.; Goodson, K.; Dai, H. Thermal conductance of an individual single-wall carbon nanotube above room temperature. *Nano Lett.* **2006**, *6*, 96–100.

6. Hergué, N.; Ernould, B.; Minoia, A.; De Winter, J.; Gerbaux, P.; Lazzaroni, R.; Gohy, J.-F.; Dubois, P.; Coulembier, O. Diblock copolymers consisting of a redox polymer block based on a stable radical linked to an electrically conducting polymer block as cathode materials for organic radical batteries. *Polym. Chem.* **2019**, *10*, 2570–2578.

7. Araya-Hermosilla, R.; Pucci, A.; Raffa, P.; Santosa, D.; Pescarmona, P.P.; Gengler, R.Y.N.; Rudolf, P.; Moreno-Villoslada, I.; Picchioni, F. Electrically-responsive reversible Polyketone/MWCNT network through Diels-Alder chemistry. *Polymers (Basel).* **2018**, *10*, 1076.

8. Anantha-Iyengar, G.; Shanmugasundaram, K.; Nallal, M.; Lee, K.P.; Whitcombe, M.J.; Lakshmi, D.; Sai-Anand, G. Functionalized conjugated polymers for sensing and molecular imprinting applications. *Prog. Polym. Sci.* 2019, *88*, 1–129.

9. Tans, S.J.; Verschueren, A.R.M.; Dekker, C. Room-temperature transistor based on a single carbon nanotube. *Nature* **1998**, *393*, 49–52.

10. Dai, L.; Chang, D.W.; Baek, J.B.; Lu, W. Carbon nanomaterials for advanced energy conversion and storage. *Small* 2012, *8*, 1130–1166.

11. Wu, Z.; Chen, Z.; Du, X.; Logan, J.M.; Sippel, J.; Nikolou, M.; Kamaras, K.; Reynolds, J.R.; Tanner, D.B.; Hebard, A.F.; et al. Transparent, conductive carbon nanotube films. *Science* **2004**, *305*, 1273–6.

12. Liu, A.; Watanabe, T.; Honma, I.; Wang, J.; Zhou, H. Effect of solution pH and ionic strength on the stability of poly(acrylic acid)-encapsulated multiwalled carbon nanotubes aqueous dispersion and its application for NADH sensor. *Biosens. Bioelectron.* **2006**, *22*, 694–699.

13. Migliore, N.; Polgar, L.; Araya-Hermosilla, R.; Picchioni, F.; Raffa, P.; Pucci, A. Effect of the Polyketone Aromatic Pendent Groups on the Electrical Conductivity of the Derived MWCNTs-Based Nanocomposites. *Polymers (Basel).* **2018**, *10*, 618.

14. Di Sacco, F.; Pucci, A.; Raffa, P. Versatile Multi-Functional Block Copolymers Made by Atom Transfer Radical Polymerization and Post-Synthetic Modification: Switching from Volatile Organic Compound Sensors to Polymeric Surfactants for Water Rheology Control via Hydrolysis. *Nanomaterials* **2019**, *9*, 458.

15. Fernandes, R.M.F.; Abreu, B.; Claro, B.; Buzaglo, M.; Regev, O.; Furó, I.; Marques, E.F. Dispersing Carbon Nanotubes with Ionic Surfactants under Controlled Conditions: Comparisons and Insight.

Langmuir **2015**, *31*, 10955–10965.

16. Koh, B.E. Dispersion of Single-Walled Carbon Nanotubes (SWCNTs) in Aqueous Solution and Reversion of SWCNT Aggregates, 2013.

17. Huang, Y.Y.; Terentjev, E.M. Dispersion of Carbon Nanotubes: Mixing, Sonication, Stabilization, and Composite Properties. *Polymers (Basel).* **2012**, *4*, 275–295.

18. Kang, Y.; Taton, T.A. Micelle-encapsulated carbon nanotubes: A route to nanotube composites. *J. Am. Chem. Soc.* **2003**, *125*, 5650–5651.

19. Stevens, J.L.; Huang, A.Y.; Peng, H.; Chiang, I.W.; Khabashesku, V.N.; Margrave, J.L. Sidewall amino-functionalization of single-walled carbon nanotubes through fluorination and subsequent reactions with terminal diamines. *Nano Lett.* **2003**, *3*, 331–336.

20. Kong, H.; Gao, C.; Yan, D. Constructing amphiphilic polymer brushes on the convex surfaces of multi-walled carbon nanotubes by in situ atom transfer radical polymerization. *J. Mater. Chem.* **2004**, *14*, 1401.

21. Kong, H.; Gao, C.; Yan, D. Controlled Functionalization of Multiwalled Carbon Nanotubes by in Situ Atom Transfer Radical Polymerization. *J. Am. Chem. Soc.* **2004**, *126*, 412–413.

22. Jeon, I.-Y.; Chang, D.W.; Kumar, N.A.; Baek, J.-B. Functionalization of Carbon Nanotubes. *IntechOpen* **2011**.

23. Duan, W.H.; Wang, Q.; Collins, F. Dispersion of carbon nanotubes with SDS surfactants: A study from a binding energy perspective. *Chem. Sci.* **2011**, *2*, 1407–1413.

24. Bonard, J.M.; Stora, T.; Salvetat, J.P.; Maier, F.; Stöckli, T.; Duschl, C.; Forró, L.; De Heer, W.A.; Châtelain, A. Purification and size-selection of carbon nanotubes. *Adv. Mater.* **1997**, *9*, 827–831.

25. Karajanagi, S.S.; Yang, H.; Asuri, P.; Sellitto, E.; Dordick, J.S.; Kane, R.S. Protein-assisted solubilization of single-walled carbon nanotubes. *Langmuir* **2006**, *22*, 1392–1395.

26. Jiang, R.; Liu, N.; Gao, S.; Mamat, X.; Su, Y.; Wagberg, T.; Li, Y.; Hu, X.; Hu, G. A facile electrochemical sensor based on PyTS-CNTs for simultaneous determination of cadmium and lead ions. *Sensors (Switzerland)* **2018**, *18*, 1567.

27. Fujigaya, T.; Nakashima, N. Non-covalent polymer wrapping of carbon nanotubes and the role of wrapped polymers as functional dispersants. *Sci. Technol. Adv. Mater.* 2015, *16*, 024802.

28. Noguchi, Y.; Fujigaya, T.; Niidome, Y.; Nakashima, N. Single-walled carbon nanotubes/DNA hybrids in water are highly stable. *Chem. Phys. Lett.* **2008**, *455*, 249–251.

29. Wang, L.; Zhao, Y. Functionalization of Carbon Nanotubes with Stimuli- Responsive Molecules and Polymers. *IntechOpen* **2016**.

30. Katchalsky, A.; Eisenberg, H. Molecular weight of polyacrylic and polymethacrylic acid. *J. Polym. Sci.* **1951**, *6*, 145–154.

31. Grunlan, J.C.; Liu, L.; Kim, Y.S. Tunable single-walled carbon nanotube microstructure in the liquid and solid states using poly(acrylic acid). *Nano Lett.* **2006**, *6*, 911–915.

32. Etika, K.C.; Cox, M.A.; Grunlan, J.C. Tailored dispersion of carbon nanotubes in water with pH-responsive polymers. *Polymer (Guildf).* **2010**, *51*, 1761–1770.

33. Grunlan, J.C.; Liu, L.; Regev, O. Weak polyelectrolyte control of carbon nanotube dispersion in water. *J. Colloid Interface Sci.* **2008**, *317*, 346–349.

34. Saint-Aubin, K.; Poulin, P.; Saadaoui, H.; Maugey, M.; Zakri, C. Dispersion and film-forming properties of poly(acrylic acid)-stabilized carbon nanotubes. *Langmuir* **2009**, *25*, 13206–13211.

35. Raffa, P.; Stuart, M.C.A.; Broekhuis, A.A.; Picchioni, F. The effect of hydrophilic and hydrophobic block length on the rheology of amphiphilic diblock Polystyrene-b-Poly(sodium methacrylate) copolymers prepared by ATRP. *J. Colloid Interface Sci.* **2014**, *428*, 152–161.

36. Raffa, P.; Brandenburg, P.; Wever, D.A.Z.; Broekhuis, A.A.; Picchioni, F. Polystyrene-poly(sodium methacrylate) amphiphilic block copolymers by ATRP: Effect of structure, pH, and ionic strength on rheology of aqueous solutions. *Macromolecules* **2013**, *46*, 7106–7111.

37. Raffa, P. Polystyrene-based amphiphilic block copolymers: Synthesis, properties and applications. In *Polystyrene: Synthesis, Characteristics and Applications*; Nova Science Publishers, 2014; pp. 31–52 ISBN 9781633213715 | 9781633213562.

38. Meijerink, M.; Mastrigt, F. van; Franken, L.E.; Stuart, M.C.A.; Picchioni, F.; Raffa, P. Triblock copolymers of styrene and sodium methacrylate as smart materials: synthesis and rheological characterization. *Pure Appl. Chem.* **2017**, *89*, 1641–1658.

39. Kang, Y.; Taton, T.A. Micelle-encapsulated carbon nanotubes: A route to nanotube composites. *J. Am. Chem. Soc.* **2003**, *125*, 5650–5651.

40. Swift, T.; Swanson, L.; Geoghegan, M.; Rimmer, S. The pH-responsive behaviour of poly(acrylic acid) in aqueous solution is dependent on molar mass. *Soft Matter* **2016**, *12*, 2542–2549.

41. Davis, K.A.; Matyjaszewski, K. Atom transfer radical polymerization of tert-butyl acrylate and preparation of block copolymers. *Macromolecules* **2000**, *33*, 4039–4047.

42. Tsarevsky, N. V.; Pintauer, T.; Matyjaszewski, K. Deactivation efficiency and degree of control over polymerization in ATRP in protic solvents. *Macromolecules* **2004**, *37*, 9768–9778.

43. Ripin, D.H.; Evans, D.A. Evans pKa Table Available online: http://www.chem.wisc.edu/areas/reich/pkatable/index.htm (accessed on Jul 8, 2019).

44. Vaisman, L.; Wagner, H.D.; Marom, G. The role of surfactants in dispersion of carbon nanotubes. *Adv. Colloid Interface Sci.* **2006**, *128–130*, 37–46.

45. Hoffmann, H.; Kamburova, K.; Maeda, H.; Radeva, T. Investigation of pH dependence of poly(acrylic acid) conformation by means of electric birefringence. *Colloids Surfaces A Physicochem. Eng. Asp.* **2010**, *354*, 61–64.

46. Mintis, D.G.; Mavrantzas, V.G. Effect of pH and Molecular Length on the Structure and Dynamics of Short Poly(acrylic acid) in Dilute Solution: Detailed Molecular Dynamics Study. *J. Phys. Chem. B* **2019**, *123*, 4204–4219.

47. Laguecir, A.; Ulrich, S.; Labille, J.; Fatin-Rouge, N.; Stoll, S.; Buffle, J. Size and pH effect on electrical and conformational behavior of poly(acrylic acid): Simulation and experiment. *Eur. Polym. J.* **2006**, *42*, 1135–1144.

48. Balberg, I.; Azulay, D.; Toker, D.; Millo, O. Percolation and tunneling in composite materials. *Int. J. Mod. Phys. B* **2004**, *18*, 2091–2121.

49. Stauffer, D.; Aharony, A. *Introduction to percolation theory*; 1994; ISBN 9780748402533.

50. Salazar, P.F.; Chan, K.J.; Stephens, S.T.; Cola, B.A. Enhanced Electrical Conductivity of Imidazolium-Based Ionic Liquids Mixed with Carbon Nanotubes: A Spectroscopic Study. *J. Electrochem. Soc.* **2014**, *161*, H481–H486.

51. Alvarenga, J.; Jarosz, P.R.; Schauerman, C.M.; Moses, B.T.; Landi, B.J.; Cress, C.D.; Raffaelle, R.P. High conductivity carbon nanotube wires from radial densification and ionic doping. *Appl. Phys. Lett.* **2010**, *97*, 182106.

52. Fujita, S.; Suzuki, A. Theory of temperature dependence of the conductivity in carbon nanotubes. *J. Appl. Phys.* **2010**, *107*, 013711.

53. Araya-Hermosilla, R.; Pucci, A.; Araya-Hermosilla, E.; Pescarmona, P.P.; Raffa, P.; Polgar, L.M.; Moreno-Villoslada, I.; Flores, M.; Fortunato, G.; Broekhuis, A.A.; et al. An easy synthetic way to exfoliate and stabilize MWCNTs in a thermoplastic pyrrole-containing matrix assisted by hydrogen bonds. *RSC Adv.* **2016**, *6*, 85829–85837.

54. Wu, S.; Li, F.; Zhu, Y.; Shen, J. The switch-type humidity sensing properties of polyacrylic acid and its copolymers. *J. Mater. Sci.* **2000**, *35*, 2005–2008.

55. Yadav, V.; Harkin, A. V; Robertson, M.L.; Conrad, J.C. Hysteretic memory in pH-response of water contact angle on poly(acrylic acid) brushes. *Soft Matter* **2016**, *12*, 3589–3599.

56. Cranford, S.W.; Buehler, M.J. Variation of Weak Polyelectrolyte Persistence Length through an Electrostatic Contour Length. *Macromolecules* **2012**, *45*, 8067–8082.

57. Misra, D.N. Adsorption of Polyacrylic Acids and Their Sodium Salts on Hydroxyapatite: Effect of Relative Molar Mass. *J. Colloid Interface Sci.* **1996**, *181*, 289–296.